Supplementary Figures

Multiplexed 3D Analysis of Immune States and Niches in Human Tissue

Clarence Yapp[1,2,*], Ajit J. Nirmal[1,2,3,*], Felix Zhou[4], Zoltan Maliga[1], Juliann B. Tefft[1,2,], Paula Montero Llopis[5], George F Murphy[6], Christine G Lian[6], Gaudenz Danuser[4], Sandro Santagata[1,2,6,7] and Peter K. Sorger[1,2,7,†]

Human Tumour Atlas Network

[1]Laboratory of Systems Pharmacology, Harvard Medical School, Boston, MA, 02115, USA.

[2]Ludwig Center at Harvard, Harvard Medical School, Boston, MA, 02115, USA.

[3]Department of Dermatology, Brigham and Women's Hospital, Harvard Medical School, Boston, MA, 02115, USA.

[4]Lyda Hill Department of Bioinformatics, UT Southwestern Medical Center, Dallas, TX, 75390, USA.

[5]Microscopy Resources on the North Quad (MicRoN), Harvard Medical School, Boston, MA 02115, USA.

[6]Department of Pathology, Brigham and Women's Hospital, Harvard Medical School, Boston, MA, 02115, USA.

[7]Department of Systems Biology, Harvard Medical School, 200 Longwood Avenue, Boston, MA 02115, USA.

*Authors contributed equally

†Corresponding Author; peter_sorger@hms.harvard.edu

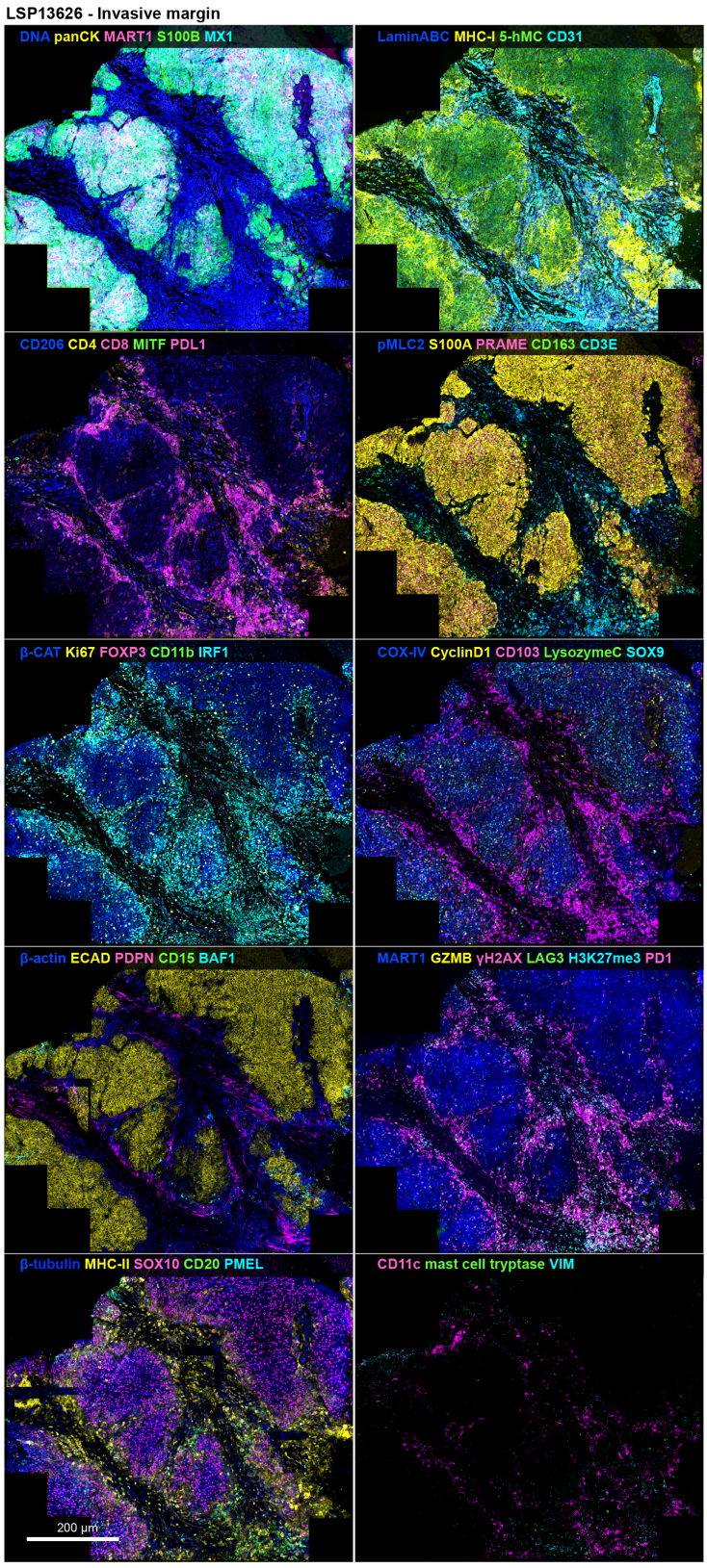

Supplementary Figure 1. Z-projection of full dataset for invasive melanoma (vertical growth phase; VGP) region for tissue section LSP13626.

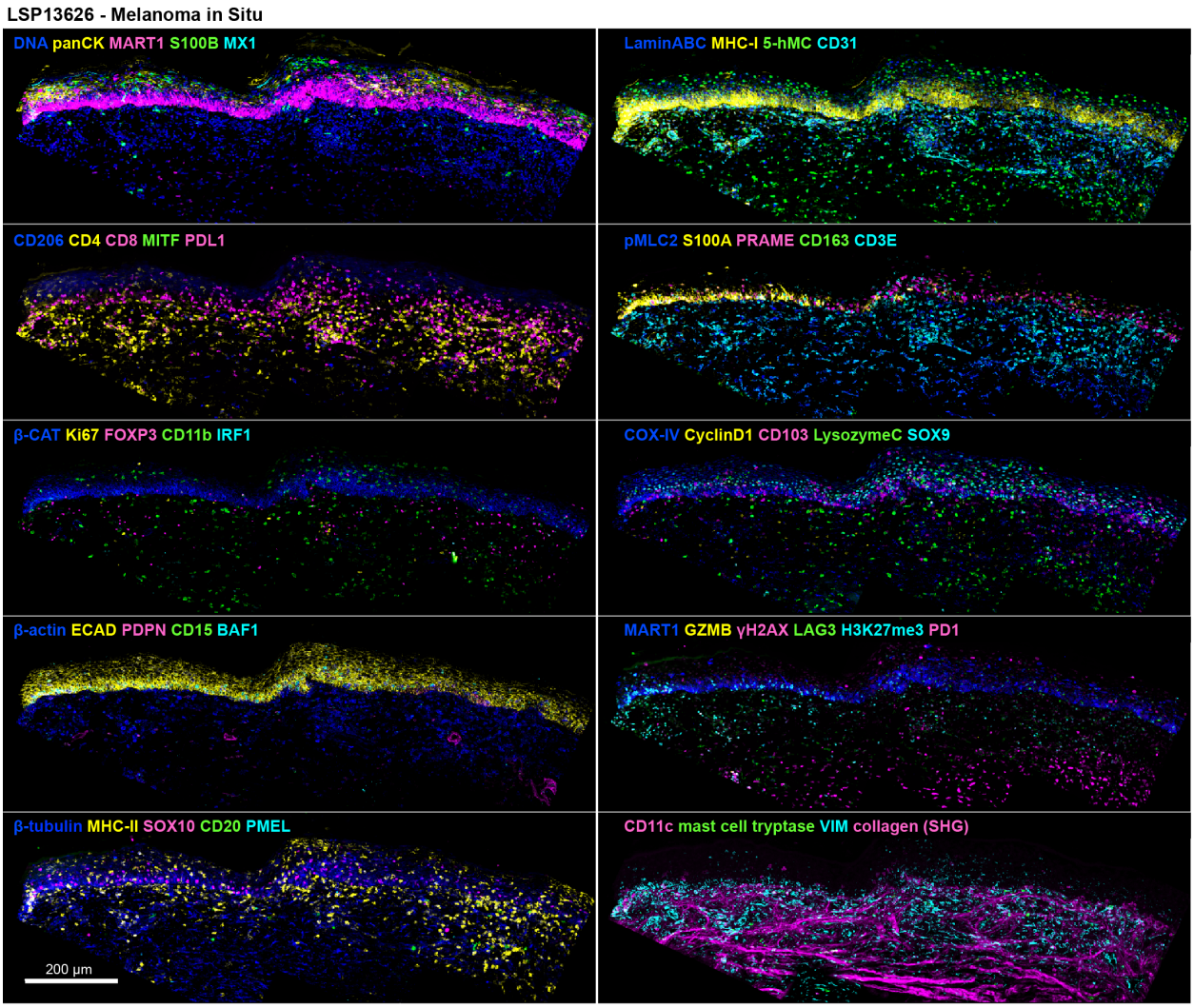

Supplementary Figure 2. Z-projection of full dataset for melanoma in situ (MIS) region for tissue section LSP13626.

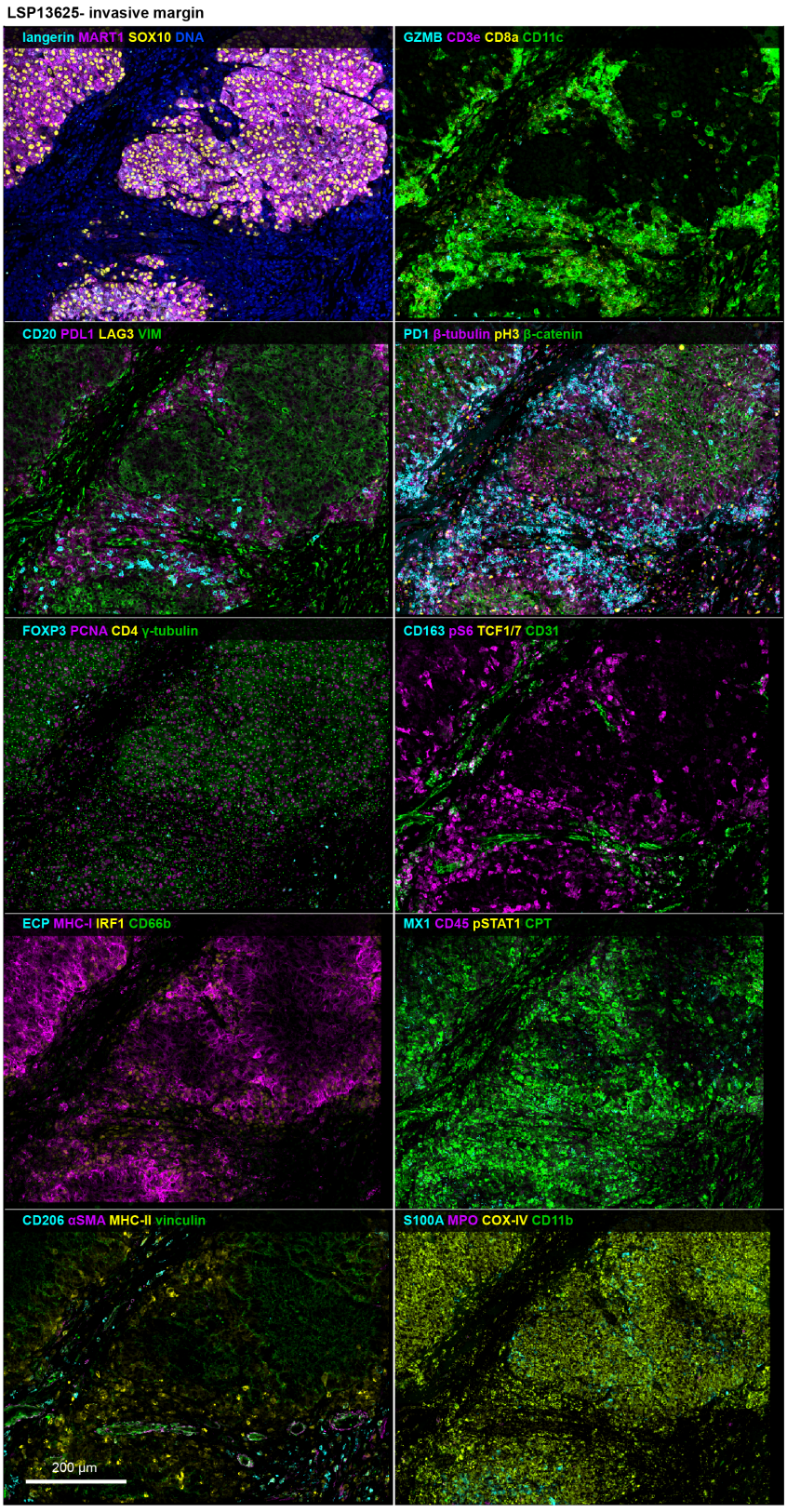

Supplementary Figure 3. Z-projection of full dataset for invasive melanoma (vertical growth phase; VGP) region for tissue section LSP13625.

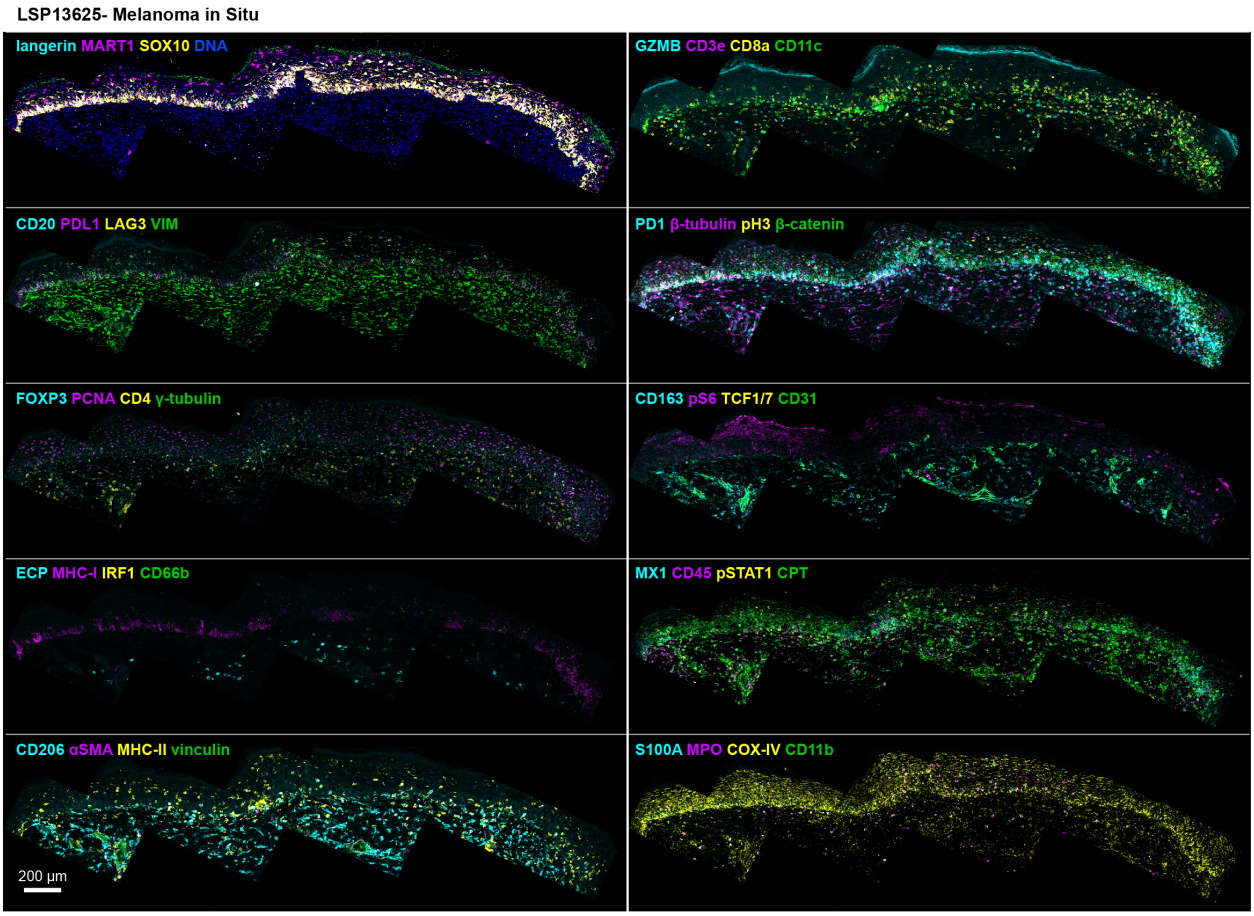

Supplementary Figure 4. Z-projection of full dataset for melanoma in situ (MIS) region for tissue section LSP13625.

LSP22409 - metastatic melanoma

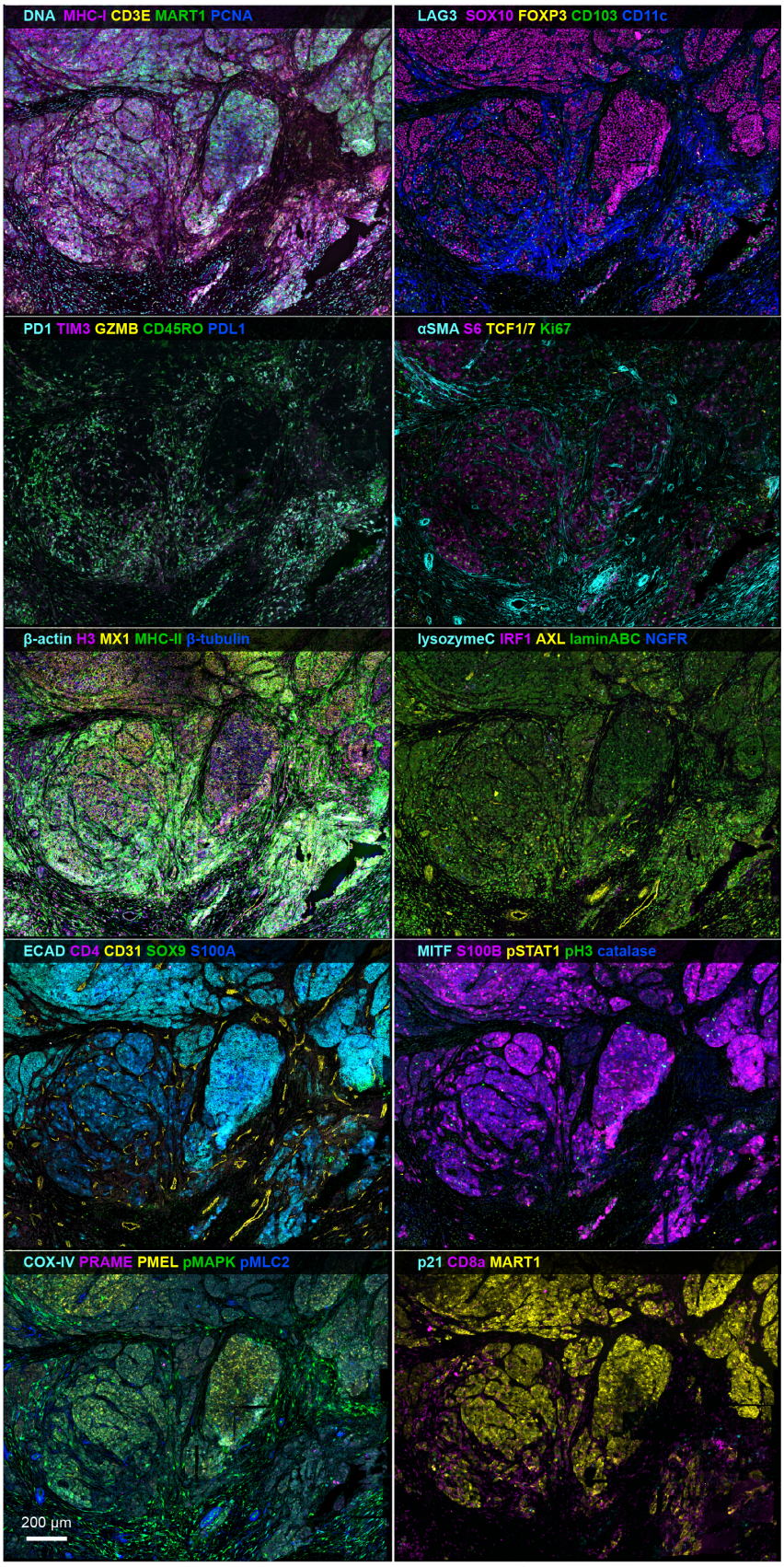

Supplementary Figure 5. Z-projection of full dataset for metastatic melanoma (tissue section LSP22409).

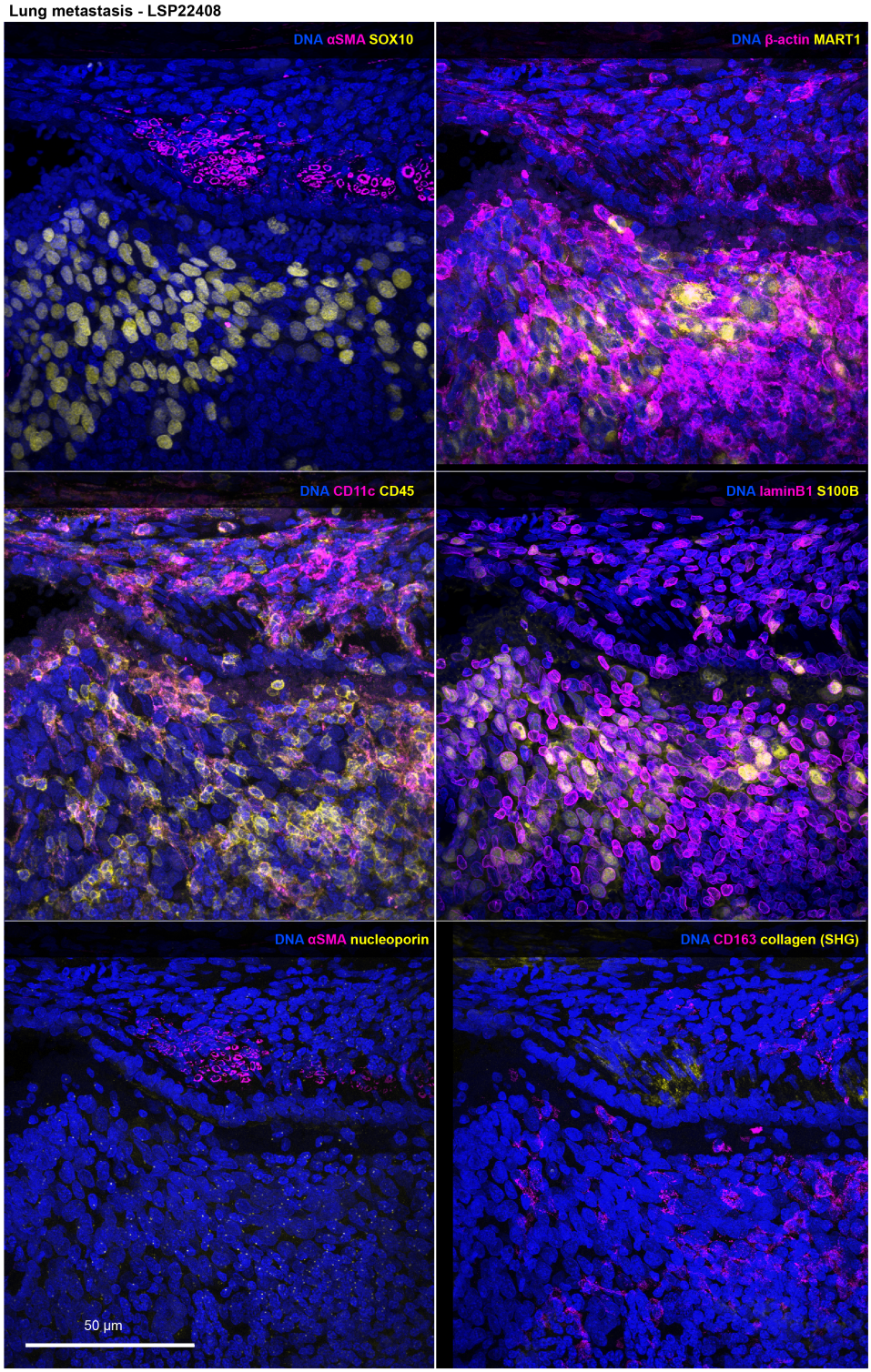

Supplementary Figure 6. Z-projection of full dataset for lung metastasis (tissue section LSP22408).

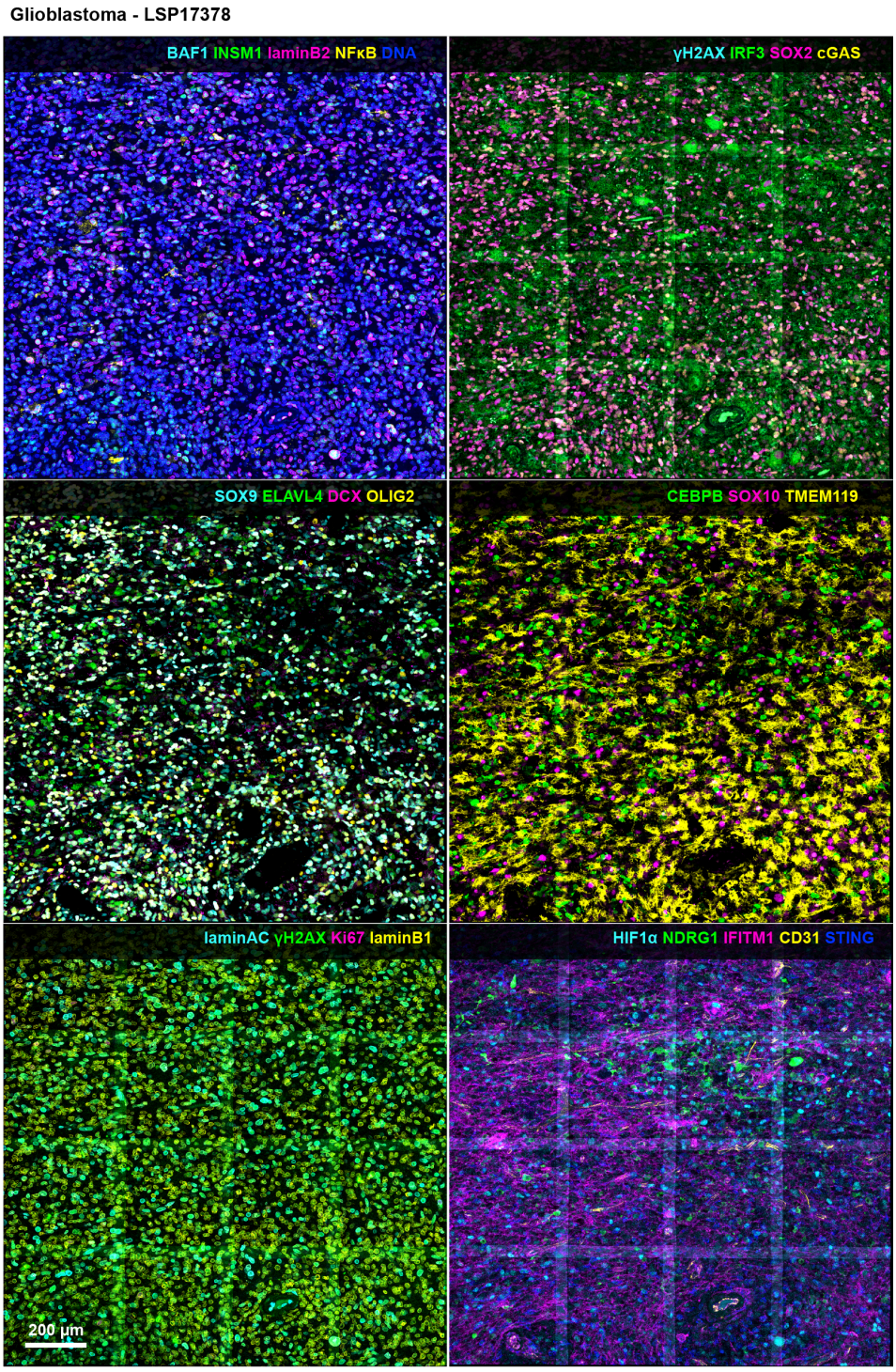

Supplementary Figure 7. Z-projection of full dataset for glioblastoma (tissue section LSP17378).

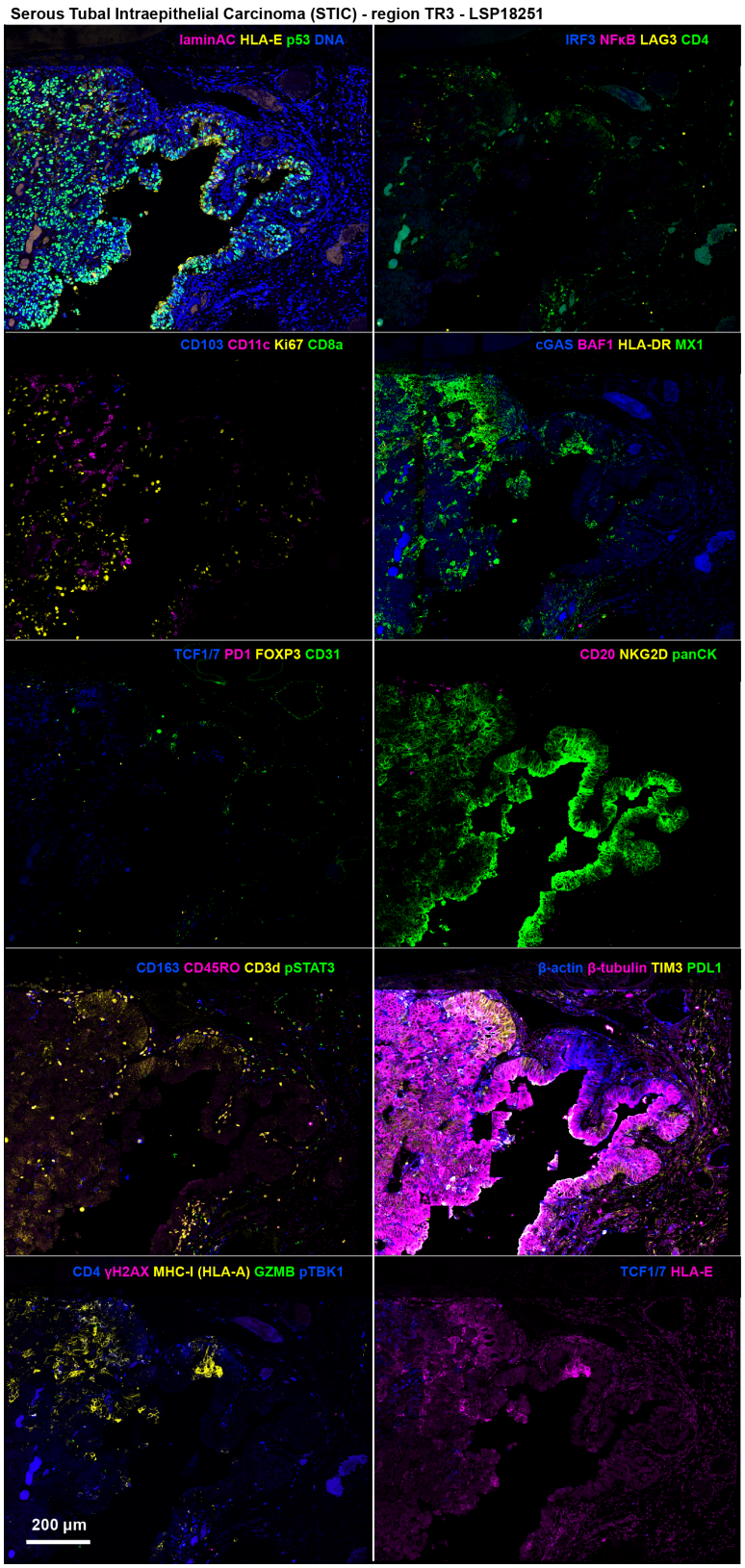

Supplementary Figure 8. Z-projection of full dataset for serous tubal intraepithelial carcinoma (STIC), region TR3 (tissue section LSP18251).

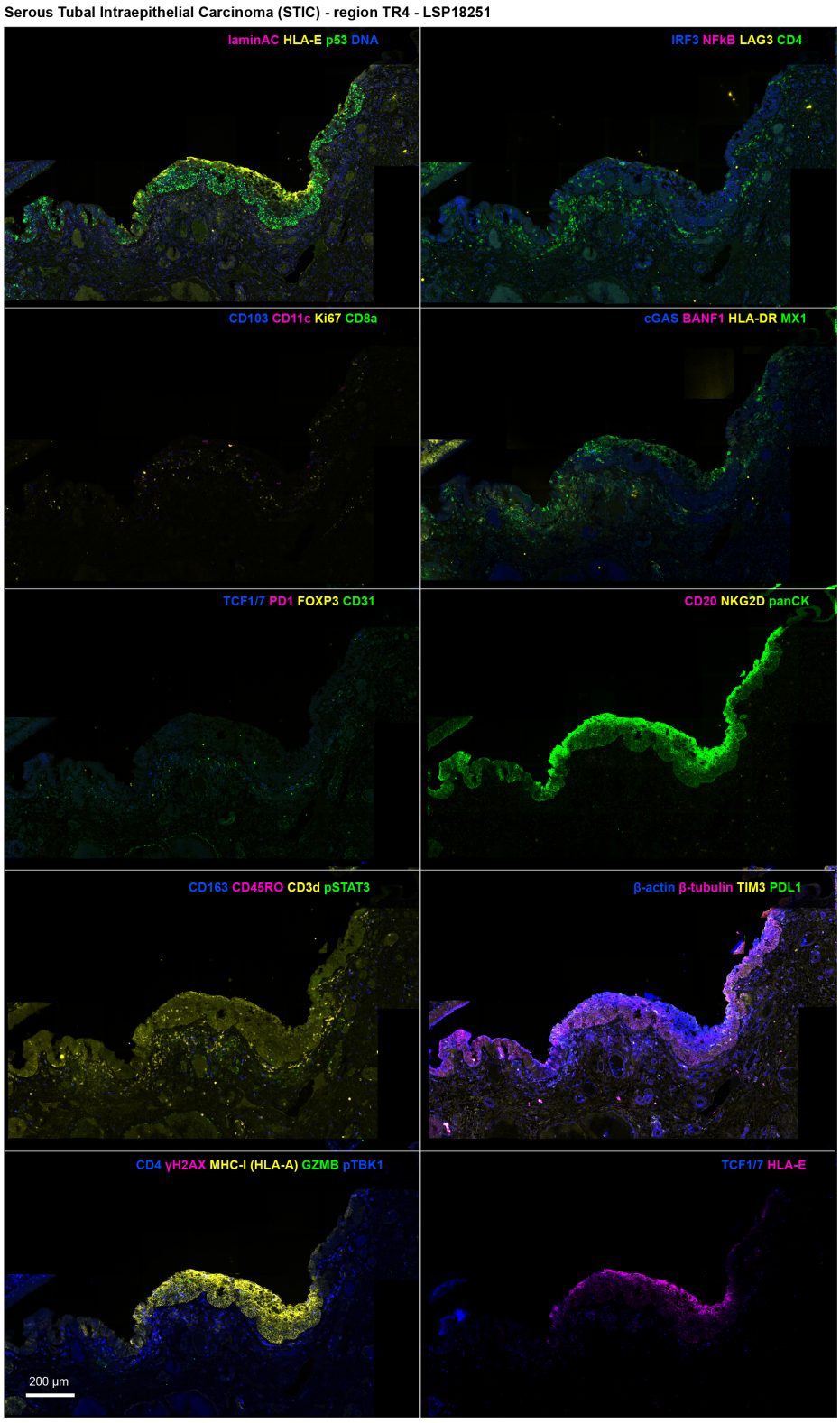

Supplementary Figure 9. Z-projection of full dataset for serous tubal intraepithelial carcinoma (STIC), region TR4 (tissue section LSP18251).

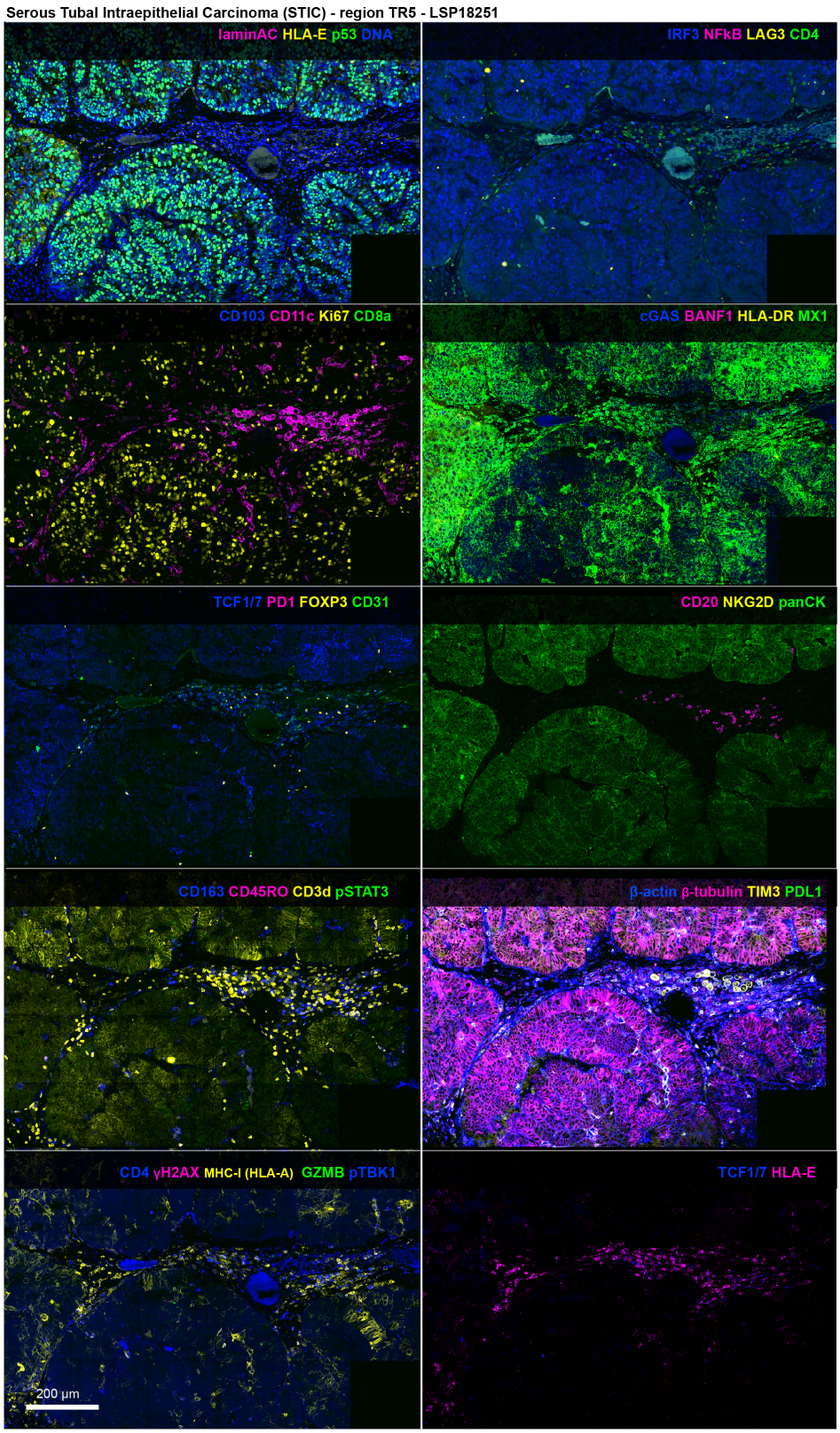

Supplementary Figure 10. Z-projection of full dataset for serous tubal intraepithelial carcinoma (STIC), region TR5 (tissue section LSP18251).

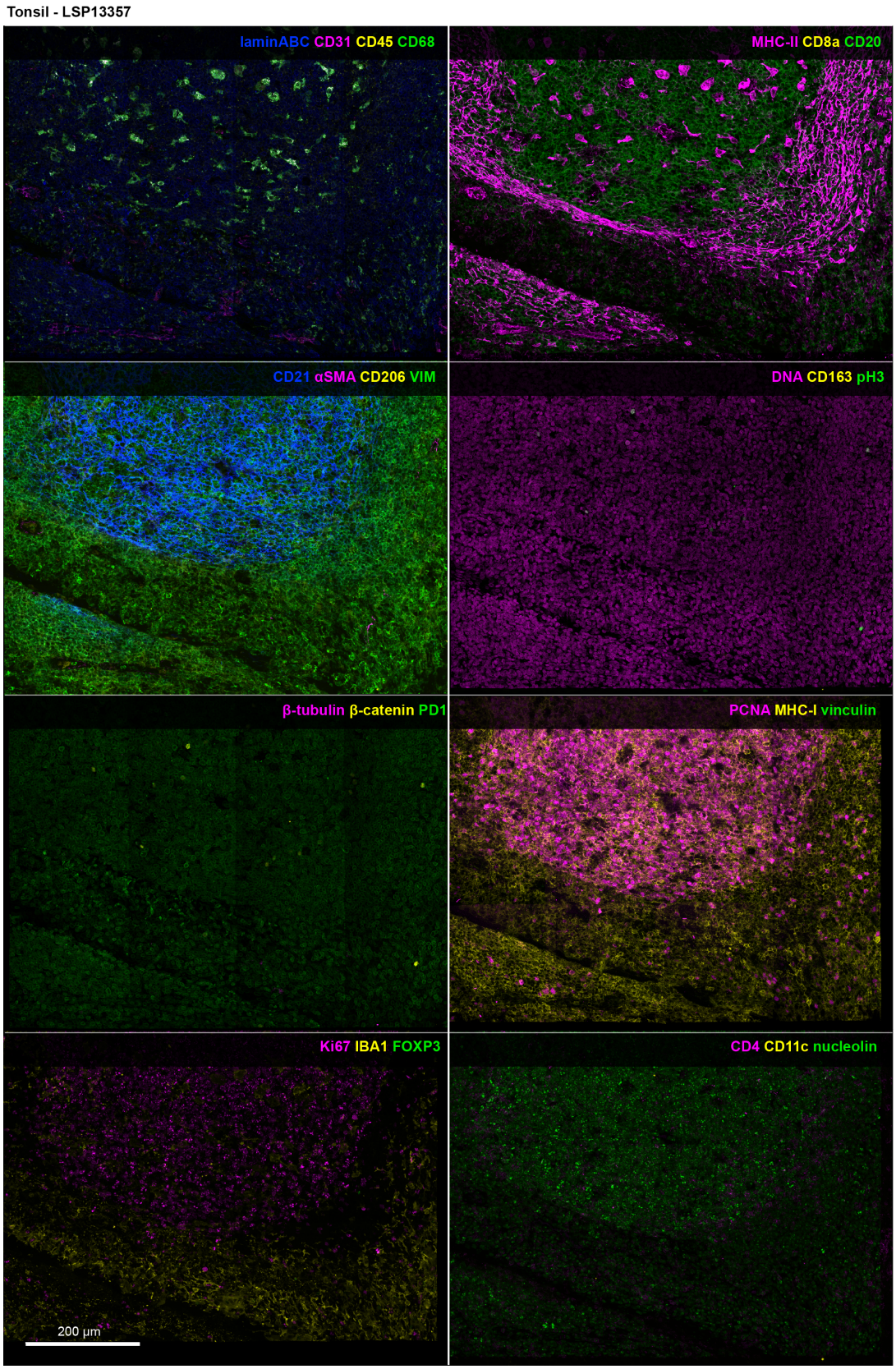

Supplementary Figure 11. Z-projection of full dataset of tonsil (tissue section LSP13357).

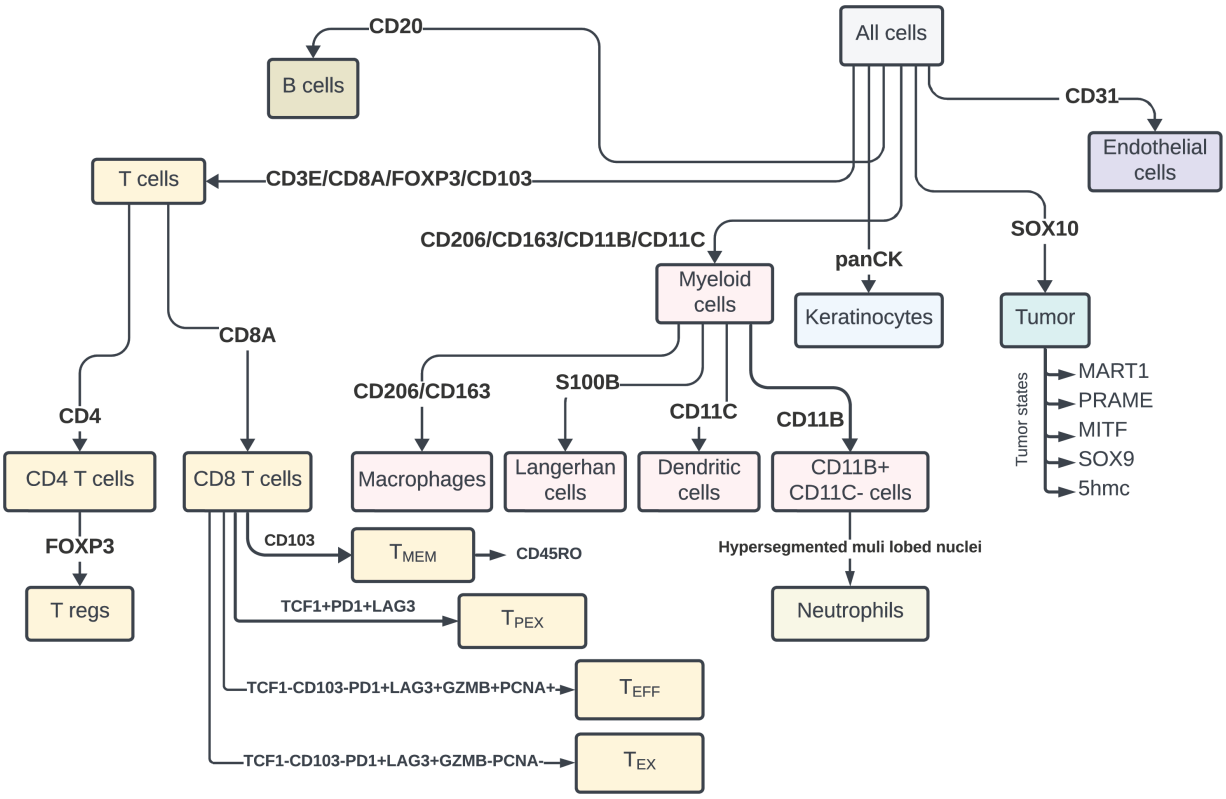

Additional markers that were used to determine cell states and morphologies:

COX-IV	CyclinD1	MX1	pMLC2	β-actin
γH2AX	KI67	IRF1	VIM	β-catenin
	PCNA	pSTAT1	Vinculin	β-tubulin

Supplementary Figure 12. Flowchart used for cell type calling in melanoma. Lines and arrows represent cells that stain positive for the indicated markers. Under tumour cells, specific tumour cell states are shown. Cell states that are not related to a specific marker are shown in the lower box.

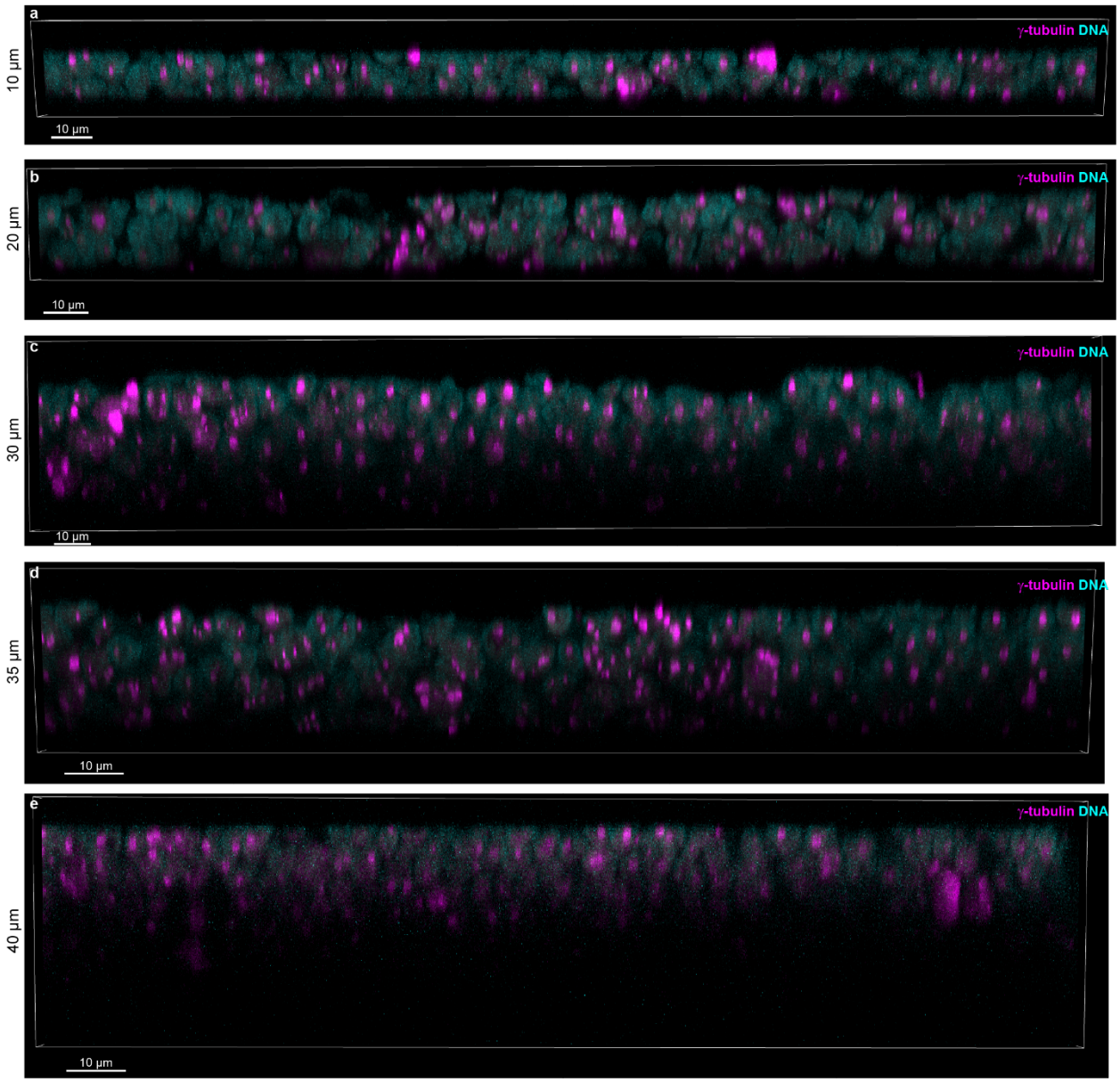

Supplementary Figure 13. Antibody penetration in tissues of different thicknesses. a-e, Orthogonal views of γ-tubulin staining (magenta) tissues of 10 µm (**a**), 20 µm (**b**), 30 µm (**c**), 35 µm (**d**), and 40 µm (**e**) thicknesses, respectively. DNA, stained with Hoechst, shown in cyan. Scalebar 10 µm.

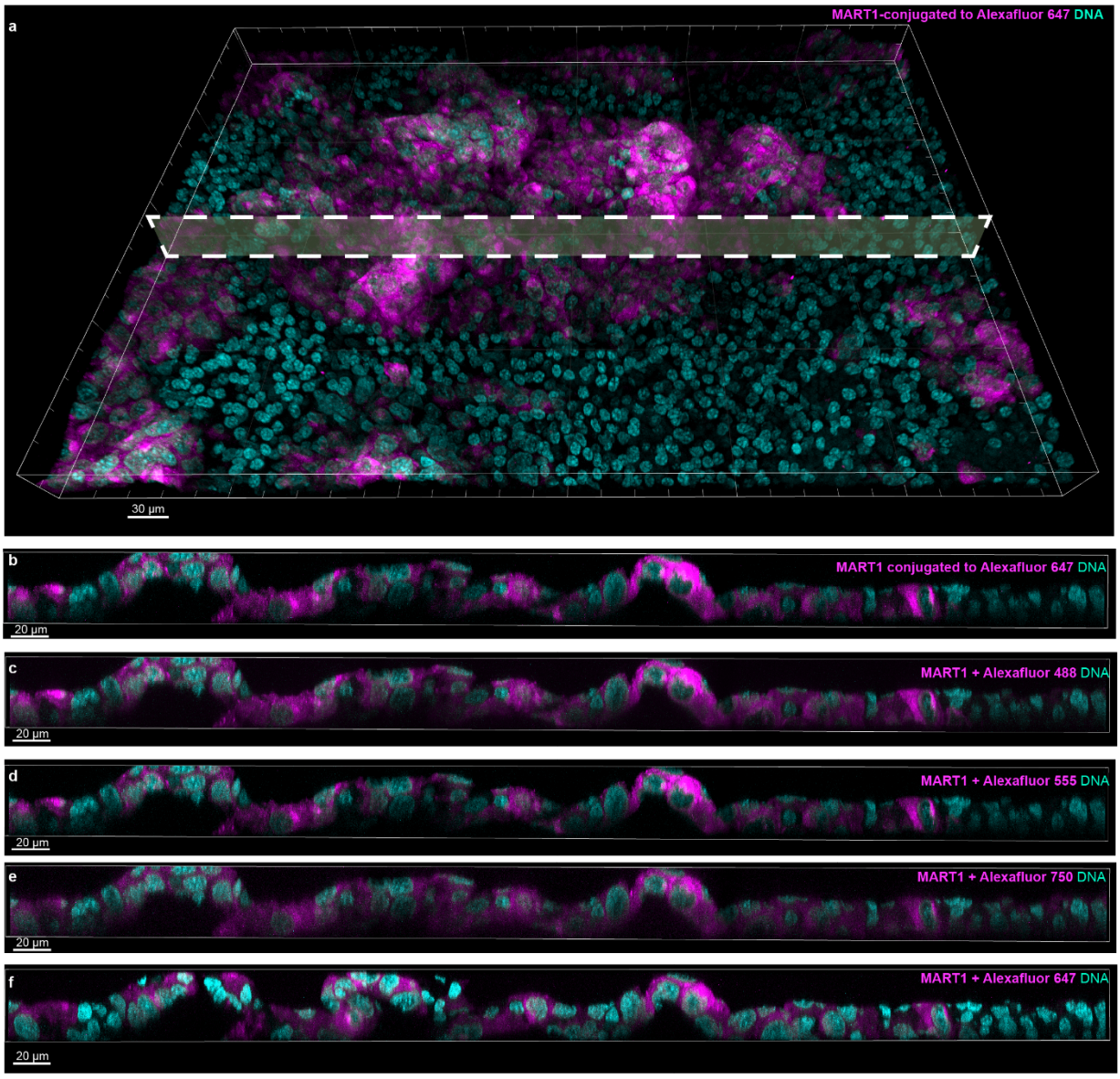

Supplementary Figure 14. Comparison of antibody penetration with different secondary antibodies against a MART1 primary conjugate. a, Volume rendering of primary melanoma, with dashed white rectangle indicating the location of the orthogonal views in **b-f**. Scale bar 30 µm. **b-f,** MART1-conjugated to Alexafluor 647 (**b**) Alexafluor 488 (**c**), Alexafluor 555 (**d**), Alexafluor 750 (**e**), or Alexafluor 647 (**f**). All combinations except MART1 + Alexafluor 647 were stained in the same cycle. MART1 + Alexafluor 647 was stained on the next cycle at the same location and same tissue specimen. Scale bars 20 µm.

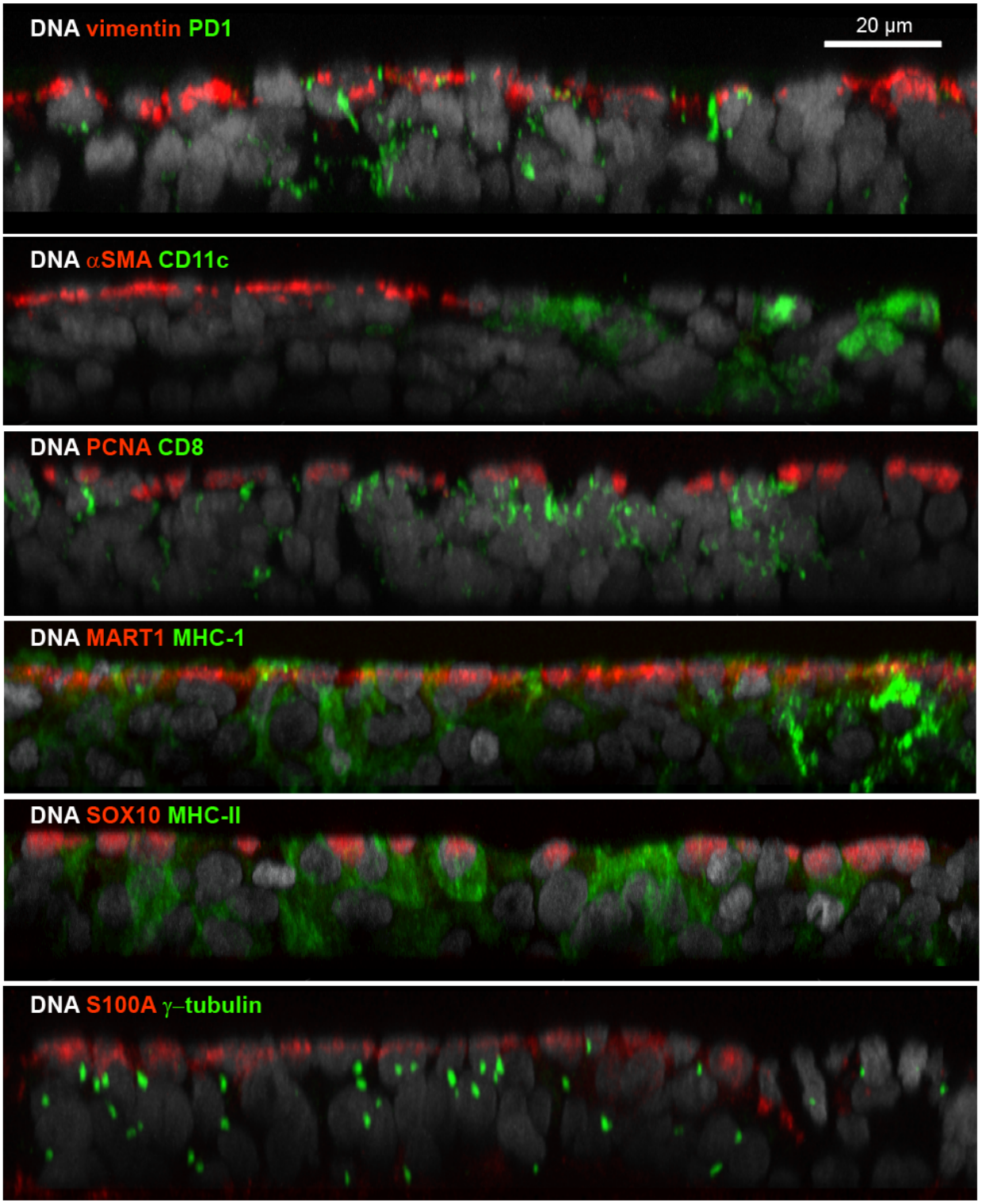

Supplementary Figure 15. Orthogonal views comparing penetration of different antibodies in the same 35-micron thick tissue section. Various antibodies (red) exhibit poor antibody penetration whereas other antibodies (green) penetrate the full thickness of tissue. DNA stained with Hoechst shown in grey. Scalebar 20 µm.

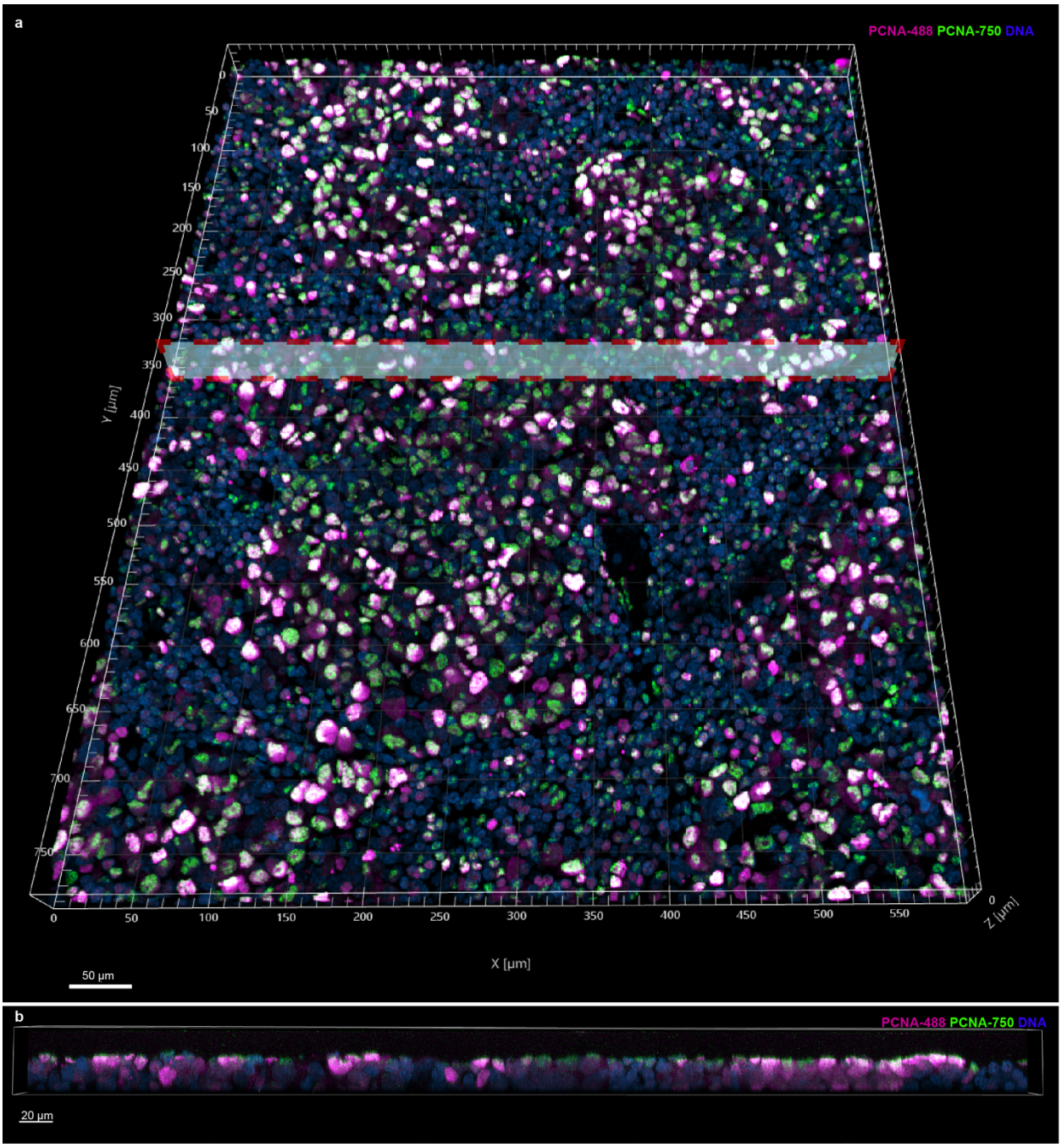

Supplementary Figure 16. Antibody penetration comparison of PCNA conjugated with Alexafluor 488 and Alexafluor 750. a, Volumetric rendering of 35 µm thick primary melanoma. Dashed red rectangle indicates location of orthogonal view in **b**. Scalebar 50 µm. **b,** PCNA-488 (magenta) penetrates tissue more deeply than PCNA-750 (green). Scalebar 20 µm.

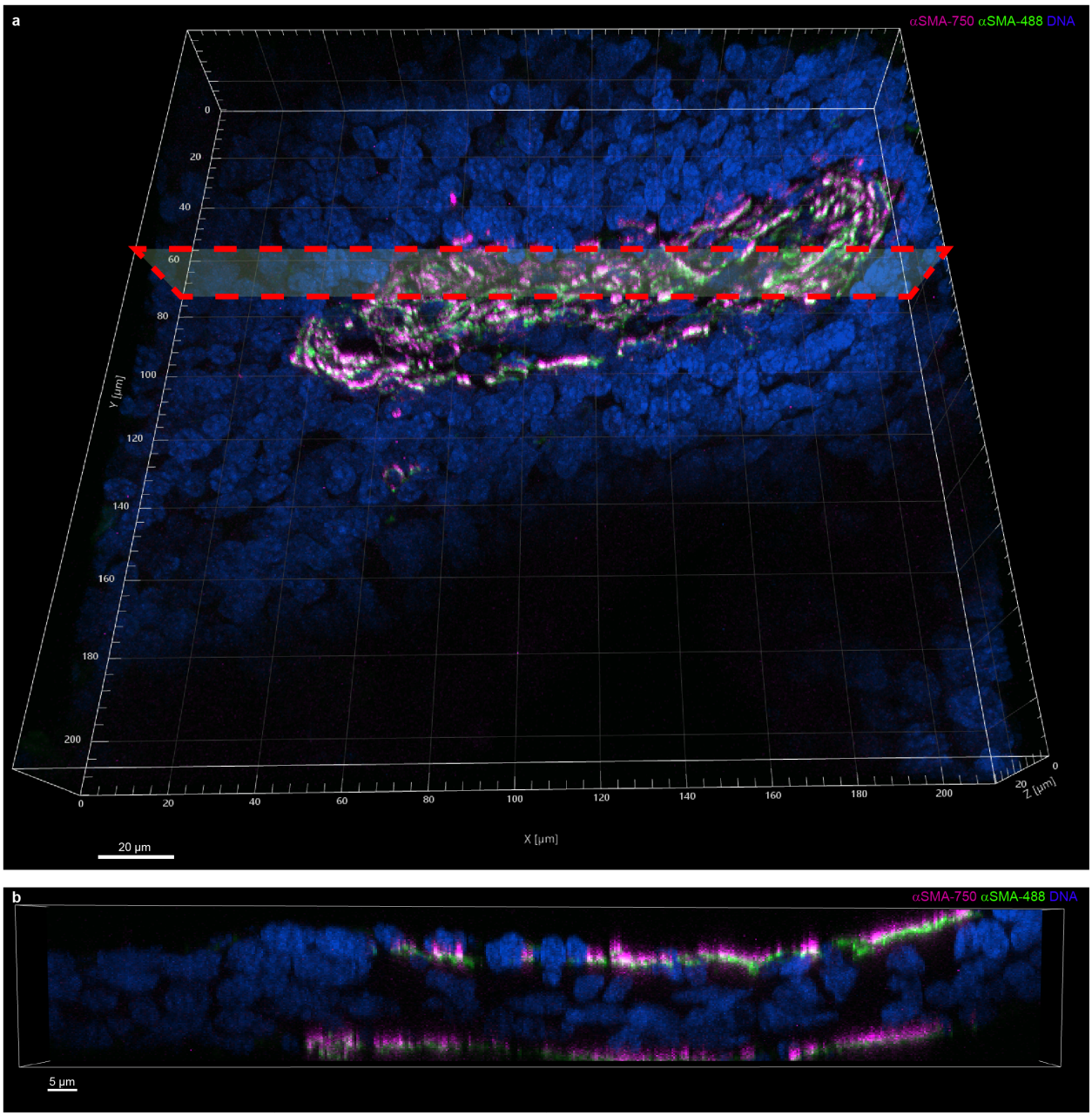

Supplementary Figure 17. Antibody penetration comparison of αSMA conjugated with Alexafluor 488 and Alexafluor 750. a, Volumetric rendering of primary melanoma with dashed red rectangle indicating location of orthogonal view in **b**. Scalebar 20 µm. **b,** Cross-sectional view of tissue. Both αSMA antibodies stain only the surface of the tissue. Scalebar 5 µm.